Regenerative Therapy 18 (2021) 66–75

Contents lists available at ScienceDirect

Regenerative Therapy

journal homepage: http://www.elsevier.com/locate/reth

Original Article

Assessment of human bioengineered cardiac tissue function in hypoxic and re-oxygenized environments to understand functional recovery in heart failure

Yu Yamasaki [a], Katsuhisa Matsuura [a, b, *], Daisuke Sasaki [a], Tatsuya Shimizu [a]

[a] Institute of Advanced Biomedical Engineering and Science, Tokyo Women's Medical University, Tokyo, Japan
[b] Department of Cardiology, Tokyo Women's Medical University, Tokyo, Japan

ARTICLE INFO

Article history:
Received 31 December 2020
Received in revised form
9 March 2021
Accepted 21 March 2021

Keywords:
Human induced pluripotent stem cells
Cardiac cell sheet
Contractile force
Hypoxia
Re-oxygenation
Heart failure

ABSTRACT

Introduction: Myocardial recovery is one of the targets for heart failure treatment. A non-negligible number of heart failure with reduced ejection fraction (EF) patients experience myocardial recovery through treatment. Although myocardial hypoxia has been reported to contribute to the progression of heart failure even in non-ischemic cardiomyopathy, the relationship between contractile recovery and re-oxygenation and its underlying mechanisms remain unclear. The present study investigated the effects of hypoxia/re-oxygenation on bioengineered cardiac cell sheets-tissue function and the underlying mechanisms.

Methods: Bioengineered cardiac cell sheets-tissue was fabricated with human induced pluripotent stem cell derived cardiomyocytes (hiPSC-CM) using temperature-responsive culture dishes. Cardiac tissue functions in the following conditions were evaluated with a contractile force measurement system: continuous normoxia (20% O_2) for 12 days; hypoxia (1% O_2) for 4 days followed by normoxia (20% O_2) for 8 days; or continuous hypoxia (1% O_2) for 8 days. Cell number, sarcomere structure, ATP levels, mRNA expressions and Ca^{2+} transients of hiPSC-CM in those conditions were also assessed.

Results: Hypoxia (4 days) elicited progressive decreases in contractile force, maximum contraction velocity, maximum relaxation velocity, Ca^{2+} transient amplitude and ATP level, but sarcomere structure and cell number were not affected. Re-oxygenation (8 days) after hypoxia (4 days) was associated with progressive increases in contractile force, maximum contraction velocity and relaxation time to the similar extent levels of continuous normoxia group, while maximum relaxation velocity was still significantly low even after re-oxygenation. Ca^{2+} transient magnitude, cell number, sarcomere structure and ATP level after re-oxygenation were similar to those in the continuous normoxia group. Hypoxia/re-oxygenation up-regulated mRNA expression of PLN.

Conclusions: Hypoxia and re-oxygenation condition directly affected human bioengineered cardiac tissue function. Further understanding the molecular mechanisms of functional recovery of cardiac tissue after re-oxygenation might provide us the new insight on heart failure with recovered ejection fraction and preserved ejection fraction.

Abbreviations: EF, ejection fraction; HFrEF, heart failure with reduced EF; HFmrEF, heart failure with midrange EF; HFpEF, heart failure with preserved EF; hiPSC-CMs, human induced pluripotent stem cell-derived cardiomyocytes; DMEM, Dulbecco's Modified Eagle Medium; FBS, fetal bovine serum; cTnT, cardiac troponin T; *NPPA*, natriuretic peptide precursor A; ATP, adenosine triphosphate; PLN, phospholamban; SERCA, sarco/endoplasmic reticulum Ca^{2+} ATPase.

* Corresponding author. Institute of Advanced Biomedical Engineering and Science, Tokyo Women's Medical University, 8-1 Kawada-cho, Shinjuku-ku, Tokyo 162-8666, Japan.
E-mail address: matsuura.katsuhisa@twmu.ac.jp (K. Matsuura).

Peer review under responsibility of the Japanese Society for Regenerative Medicine.

https://doi.org/10.1016/j.reth.2021.03.007

1. Introduction

Heart failure affects more than 23 million people globally and is a major cause of ill health, hospitalization and death [1]. Pharmacotherapies targeting neurohormonal mechanisms have been shown to reduce morbidity and mortality in patients who have heart failure with reduced ejection fraction (EF), and the available drugs include angiotensin converting enzyme inhibitors, angiotensin receptor antagonists, mineralocorticoid receptor antagonists and beta-blockers [2,3]. Patients with heart failure can be categorized into three distinct populations based on their EF: heart failure with reduced EF (HFrEF), heart failure with midrange EF (HFmrEF) and heart failure with preserved EF (HFpEF) [4]. The 5-year mortality rate is similar among these categories [5], but whether pre-treatment EF is a predictor of prognosis remains unconfirmed. It was reported that one in four patients with HFrEF showed recovery of systolic function after treatment, and those with HFrEF and functional recovery had significantly lower mortality and morbidity than patients with HFpEF or those with HFrEF who did not exhibit recovery [6]. HFmrEF can be further subclassified as HFmrEF improved, HFmrEF unchanged and HFmrEF deteriorated, and patients with HFmrEF improved appear to have better outcomes than those in the other two categories despite similar EFs [7]. Therefore, patients who exhibit a recovery of function after treatment might be quite different to those who have unchanged or deteriorating cardiac function. However, the mechanisms underlying functional recovery are incompletely understood. Moreover, around 40% of patients with dilated cardiomyopathy relapse following the withdrawal of medical treatment despite achieving recovery to an asymptomatic state during therapy [8]. Thus, myocardium that shows functional recovery likely differs from healthy myocardium, but the differences remain uncharacterized. Further research in patients with heart failure and in suitable preclinical model systems are needed to identify the differences between diseased and healthy myocardium and facilitate the future development of new treatments to improve outcomes.

Numerous studies have evaluated human induced pluripotent stem cell (iPSC)-derived cardiomyocytes (hiPSC-CMs) as model systems for research into disease mechanisms and as novel therapies for cardiac disorders. For example, cardiac cells obtained from iPSCs have been used to investigate the proarrhythmogenic potential of drugs [9] and as models of cardiomyopathy [10,11] and viral myocarditis [12]. Importantly, recent advancements in tissue engineering technology have enabled the fabrication of two-dimensional and three-dimensional structures built around scaffolds [13,14]. An alternative approach to scaffold-based methods is to culture cells on temperature-sensitive polymer surfaces to create scaffold-free cell sheets [15–17], and the cell sheet-based technique has been used to bioengineered human cardiac tissue constructs [18,19]. Furthermore, systems have been developed to monitor contractile force and electric potential in human cardiac cell sheets [20,21]. Human cardiac tissue constructs derived from iPSCs potentially represent an excellent model system for research into heart failure. However, although one previous report described a model of ischemia-reperfusion comprising iPSC-CMs in a hydrogel scaffold [22], few studies have used iPSC-derived cardiac cells to examine how ischemia and reperfusion alter contractility and explore the mechanisms contributing to the development of heart failure.

The main aim of this study was to develop and validate a model system based on iPSC-derived cardiac cell sheets that could be used to investigate the effects of hypoxia and reoxygenation on contractile function and elucidate the underlying mechanisms.

2. Methods

2.1. Cardiomyocyte differentiation from hiPSCs and purification

iPSC line 201B7 was purchased from RIKEN (Tsukuba, Japan) [23]. hiPSCs expressing α-MHC and rex-1 promoter-driven drug-resistance genes were cultured on inactivated mouse embryonic fibroblasts (ReproCELL, Yokohama, Japan) as described previously [24]. Cardiac differentiation of hiPSCs in a stirred bioreactor system (Able, Tokyo, Japan) was achieved using a modified version of the procedure described previously [25]. Cells were harvested from cell aggregates on day 17 of differentiation using 0.05% trypsin/EDTA (Life Technologies, Carlsbad, CA, USA) and cultured in Dulbecco's Modified Eagle Medium (DMEM) supplemented with 10% fetal bovine serum (FBS) and penicillin–streptomycin (Sigma–Aldrich) at 37 °C in a humidified atmosphere with 5% CO_2. On day 21, the cells were incubated with 1.5 μg/mL puromycin (Sigma–Aldrich) for 24 h to purify the cardiomyocytes. On day 23, the remaining cells were harvested with 0.05% trypsin/EDTA and utilized for cell sheet fabrication.

2.2. Flow cytometric analysis

At the end of the purification process, the remaining cells were fixed with 4% paraformaldehyde, and the percentage of iPSC-CMs was determined with a MoFlo XDP cell sorter (Beckman Coulter, Brea, CA, USA).

2.3. Fibrin gel sheet preparation

Fibrin gel sheets were prepared as the bases of the cardiac cell sheets for measurement of contractile force. 'Handles' made of ultraviolet-curing resin (MED610; Stratasys, Eden Prairie, MN, USA) and molds formed from silicone rubber sheets were prepared as previously described [20]. Fibrin gel solution (10 mg/mL fibrinogen (F8630; Sigma–Aldrich), 0.5 units/mL thrombin (T4648; Sigma–Aldrich), 20 IU/mL Fibrogammin P I.V. Injection (CSL Behring K.K., Tokyo, Japan), 2 mmol/L $CaCl_2$, 0.025% Polyoxyethylene(20) Sorbitan Monooleate, and 154 mmol/L NaCl) was prepared by mixing stock solutions, and immediately poured into the mold in which the two handles were put at both sides. Then an acrylic plate was put on it, and the fibrin gel solution was allowed to clot for more than 20 min at room temperature. The resultant fibrin gel sheet was picked out from the mold and preserved in DMEM supplemented with 10% FBS and 500 KIU/mL aprotinin.

2.4. Cardiac cell sheet preparation for contractile force measurement

First, silicone rubber frames were sterilized and attached to the surface of temperature-responsive dishes (UpCell; CellSeed, Tokyo, Japan). The cell culture area was a 12-mm by 12-mm square, and the culture surfaces were treated with FBS overnight before the cell seeding process. iPSC-CMs were seeded at 3×10^5 cells/cm^2 (day 23) and cultured in DMEM supplemented with 10% FBS at 37 °C in a humidified atmosphere containing 5% CO_2. The medium was changed to fresh medium on day 24 and then every other day. iPSC-derived cardiac cell sheets were ready to be transferred to the surface of fibrin gel sheets on day 28, as described previously [20]. Cardiac cell sheet contractile force was measured from day 30.

2.5. Contractile force measurement

The configuration of the contractile force measurement system has been described in detail in a prior publication [20].

Briefly, the contractile force measurement device was comprised of a load cell (LVS-10GA; Kyowa Electronic Instruments, Tokyo, Japan) and a culture bath made of acrylic plates. A clip was fixed to hold the handle of a fibrin gel sheet to the bottom of the culture bath. The height of the load cell could be fine-tuned using a uniaxial stage (Chuo Precision Industrial, Tokyo, Japan). The fibrin gel sheet was suspended from the sensor rod of the load cell using a custom-made hook (Objet Eden350; Stratasys), and the lower handle of the fibrin gel sheet was held by the clip on the bottom of the culture bath. Rubber stoppers were used to close the holes at the front of the culture bath, and 40 mL Medium 199 with Hanks' Balanced Salts (Thermo Fisher Scientific, Waltham, MA, USA) containing 10% FBS, 500 KIU/mL aprotinin and penicillin–streptomycin was added to the bath. The medium was stirred gently by a magnetic bar placed in the bath. The measurement of contractile force was performed at 37 °C. The load cell was connected to a strain amplifier (DPM-912B; Kyowa Electronic Instruments), and the force was recorded by a computer through an A/D converter (Power Lab 8/30; ADInstruments, Bella Vista, Australia). The culture baths, hooks, magnetic bars and rubber stoppers were sterilized with ethylene oxide gas before use. Data were collected from different batches and pooled for the analysis.

2.6. Immunocytochemistry

To evaluate the number of cells under each condition, cells were seeded on 24-well plates (Corning, Corning, NY, USA) and incubated for 4–12 days according to the assigned conditions. Cells were fixed with 4% paraformaldehyde and subjected to immunocytochemistry as described previously [18]. Samples were imaged by ImageXpress (Molecular Devices, Sunnyvale, CA, USA). MetaXpress and Acuity software (Molecular Devices) were used for data analysis. To evaluate sarcomere structure, cells were seeded on cover-glass in 60-mm culture dishes and incubated according to the assigned experimental conditions. Nuclei were stained with Hoechst 33258 (H341, Dojindo Laboratories, Kanagawa, Japan). Samples were imaged with a BZ-9000 fluorescence microscope (Keyence Corporation, Osaka, Japan).

2.7. Ca^{2+} imaging

hiPSC-CMs at day 23 were seeded onto EZ Sphere (AGC Techno Glass, Shizuoka, Japan) at 5×10^4 cells/cm^2 to form a spheroid. The following day (day 24), spontaneous beating was confirmed, and the spheroids were moved to a normoxic (20% O_2) or hypoxic (1% O_2) incubator for 4 or 12 days to be cultured in DMEM supplemented with 10% FBS and penicillin–streptomycin (Sigma–Aldrich). The culture medium was changed every 4 days. To investigate intracellular Ca^{2+} transients, spheroids were transferred to 6-well plates and loaded with 5 μM Fluo-8 (AAT Bioquest, Sunnyvale, CA, USA) in DMEM supplemented with 10% FBS for 1 h in a humidified incubator with 5% CO_2 at 37 °C. Ten minutes before observation, each well was immersed in phenol red-free DMEM (Nacalai Tesque, Kyoto, Japan) containing 10% FBS and penicillin–streptomycin. Changes in fluorescence levels were monitored at a rate of 100 ms with an ORCA-R2 CCD camera (Hamamatsu Photonics K.K., Shizuoka, Japan) and processed with Aquacosmos image processing software (Hamamatsu Photonics K.K.) for baseline correction and colored visualization. The Ca^{2+} transient was recorded during electrical stimulation at 1 Hz (C-Pace EP, IonOptix, Westwood, MA, USA).

2.8. RNA extraction and quantitative reverse transcription-polymerase chain reaction (RT-PCR)

Total RNA was isolated using the RNeasy Micro Kit (Qiagen, Venlo, Netherlands). cDNA synthesis was carried out using the High Capacity cDNA Reverse Transcription Kit (Applied Biosystems, Stockholm, Sweden) with random hexamer primers. RT-PCR analysis of each sample was conducted with a StepOne or StepOnePlus RealTime PCR System (Applied Biosystems). TaqMan assays for RT-PCR are listed in Table 1. The average copy number of the gene transcripts was normalized to that of β-actin for each sample.

2.9. Determination of ATP level

hiPSC-CMs on day 23 of differentiation were seeded in 96-well optical-bottom plates (165306; Thermo Fisher Scientific) and cultured for 2 days (day 25). Then, the cells were incubated under normoxic (20% O_2) or hypoxic (1% O_2) conditions for the assigned periods. The cardiac tissues were equilibrated at room temperature for approximately 30 min, and then the ATP level was measured using the CellTiter-Glo Luminescent Cell Viability Assay G7570 (Promega, Madison, WI, USA). The medium was replaced with 100 μL reagent in 100 μL medium, and measurements were made using a Glomax Multi+ Detection System (Promega).

2.10. Antibodies

The following antibodies were used for flow cytometric analysis and immunocytochemistry: rabbit monoclonal anti-cTnT antibody (ab45932, Abcam, Cambridge, UK), mouse monoclonal anti α-actinin (sarcomeric) antibody (A7811, Sigma–Aldrich, St. Louis, MO, USA), phycoerythrin (PE)-conjugated mouse monoclonal anti-myosin heavy chain antibody (MF20, 564408, BD Pharmingen, Franklin Lakes, NJ, USA), and allophycocyanin (APC)-conjugated anti-cTnT antibody (130-106, Miltenyi Biotec, Bergisch Gladbach, Germany). Secondary antibodies were purchased from Jackson ImmunoResearch Laboratories (West Grove, PA, USA).

2.11. Statistical analysis

Data are presented as mean ± standard deviation. Statistical comparisons between two groups were performed using the paired or unpaired Student's *t*-test. Multiple-group comparisons were made by repeated-measures one-way analysis of variance followed by Tukey or Dunnett post-hoc tests. A *P*-value <0.05 was considered statistically significant.

Table 1
PCR primer information.

Gene name	Applied Biosystems TaqMan assay ID
ACTB	Hs99999903_m1
TNNT2	Hs00165960_m1
MYL2	Hs00166405_m1
MYL7	Hs01085598_g1
NPPA	Hs00383230_g1
NPPB	Hs01057466_g1
ATP2A2	Hs01566028_g1
PLN	Hs00160179_m1
RYR2	Hs00181461_m1
CACNA1C	Hs00167681_m1
MYH6	Hs01101425_m1
MYH7	Hs01110632_m1
COL1A1	Hs00943809_m1
COL3A1	Hs00164004_m1

3. Results

3.1. Purity of the cardiomyocytes in the cardiac cell sheet

In this study, cell sheets representing healthy cardiac tissue were bioengineered from the 201B7 human iPSC line, which contained a puromycin-resistance gene under the control of an α-myosin heavy chain (α-MHC) promoter. This enabled the iPSC-CMs to be purified by exposure to puromycin. Fig. 1A shows a representative flow cytometry histogram illustrating that most of the cells obtained after treatment with puromycin were cardiac troponin T (cTnT)-positive cardiomyocytes (72.5 ± 12.8%, $n = 8$). Based on our previous report that the non-cardiomyocyte cells present after puromycin treatment were vimentin-positive fibroblasts [19], the hiPSC-derived cardiac cell sheets used in this study were composed mainly of cardiomyocytes and fibroblasts.

3.2. Effects of hypoxia on bioengineered cardiac cell sheet function

A contractile force measurement system was used to evaluate the effects of hypoxic and re-oxygenized conditions on cardiac cell sheet function (Fig. 1B) [20]. First, we cultured hiPSC-derived cardiac cell sheets under normoxic (20% O_2) or hypoxic (1% O_2) conditions for 4 days and compared their cardiac tissue function (Fig. 1C). At the start of the experiment (D0), the monolayered cardiac cell sheet generated around 1 mN of contractile force, and the force generated did not change after 4 days of culture under normoxic conditions (Fig. 2A and B). By contrast, contractile force under hypoxic conditions was significantly decreased at day 4 (Fig. 2A and B). Furthermore, several parameters, including beating rate, contraction time, relaxation time, maximum contraction velocity and maximum relaxation velocity, were also markedly decreased after culture under hypoxic conditions (Fig. 2B). Contractile force, beating rate, maximum contraction velocity and maximum relaxation velocity at day 4 were lower in the hypoxic group than in the normoxic group (Fig. 2C), suggesting that hiPSC-derived cardiac tissue function deteriorates under hypoxic conditions.

Next, we examined the mechanisms underlying functional deterioration under hypoxic conditions. The number of cTnT-positive cells did not differ between hiPSC-CMs cultured under normoxic conditions for 4 days and those cultured under hypoxic conditions for 4 days (Fig. 3A and B). Interestingly, exposure to hypoxia for 4 days did not result in obvious changes in sarcomere structure (Fig. 3C). In line with the immunocytochemical analysis, the mRNA expression levels of cardiac genes were also not different between groups, except for natriuretic peptide precursor A (*NPPA*) (Fig. 3D). The above findings suggest that cell death or changes in the expression of cardiac contractile elements may not be responsible for the impairment of cardiac tissue function under hypoxic conditions. hiPSC-CMs subjected to hypoxia for 4 days had a significantly lower adenosine triphosphate (ATP) level than those maintained for 4 days under normoxic conditions (Fig. 3E). Moreover, the magnitude of the Ca^{2+} transient was significantly smaller in cardiomyocytes subjected to hypoxia for 4 days than in cardiomyocytes kept under normoxic conditions ($P < 0.001$; Fig. 3F and G). These findings suggest that impaired ATP production and suppression of the Ca^{2+} transient might contribute to the reduction in contractile force observed after hypoxia.

3.3. Effects of re-oxygenation on cardiac cell sheet function

Since 4-day exposure to hypoxia induced an impairment of cardiac cell sheet function accompanied by insufficient ATP production and reduced intracellular Ca^{2+} concentration, additional experiments were carried out to determine whether re-oxygenation affected bioengineered cardiac tissue function. hiPSC-derived cardiac tissues were divided into three groups and subjected to the following conditions: hypoxia for 4 days (D0–D4) followed by re-oxygenation for 8 days (D4–D12); continuous hypoxia for 12 days (D0–D12); or continuous normoxia for 12 days (D0–D12). In the continuous normoxia (control) group, contractile force and maximum contraction velocity increased progressively and contraction time decreased progressively from day 4 to day 12 (Fig. 4A and B), while relaxation time, maximum relaxation velocity and beating rate did not change during this experimental period (Fig. 4A and B). By contrast, cardiac sheets exposed to continuous hypoxia showed reductions in contractile force, maximum contraction velocity, maximum relaxation velocity and beating rate between days 4 and 8 (Fig. 4A and B), and no spontaneous contractions were detectable after 12 days of hypoxia (data not shown). In cell sheets exposed to hypoxia for 4 days followed by re-oxygenation for 8 days, re-oxygenation was associated with a progressive recovery in contractile force and maximum contraction velocity (Fig. 4A and B), although beating rate appeared to remain suppressed at day 12 (Fig. 4B). Importantly, re-oxygenation also resulted in a substantial prolongation of relaxation time from 0.26 ± 0.06 s at day 4 to 0.47 ± 0.05 s at day 12 (Fig. 4B), and

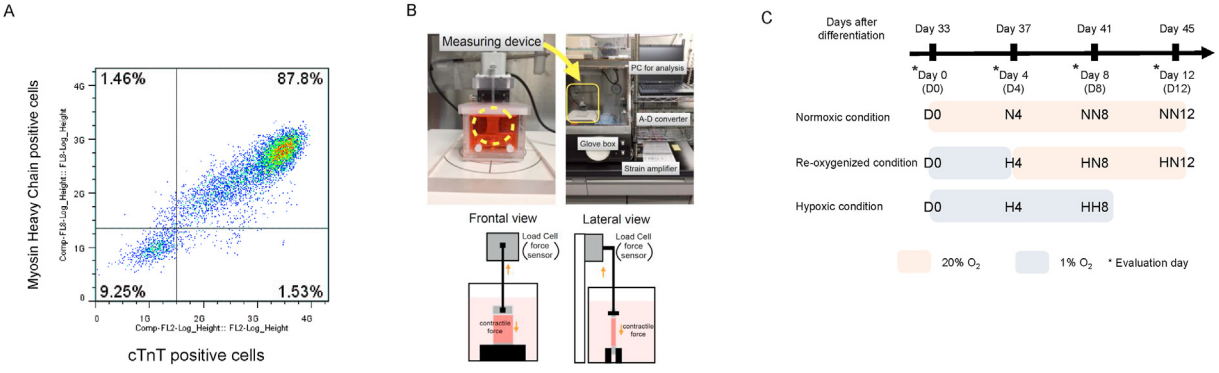

Fig. 1. Assessment of the purity of iPSC-CMs after exposure to puromycin and schematic of the experimental design. (A) Representative flow cytometry plots demonstrating the presence of cTnT-positive and myosin heavy chain-positive cardiomyocytes after puromycin treatment. (B) Upper panel: photographs showing the contractile force measurement system. Lower panel: schematic illustration of the contractile measurement system. (C) Cardiomyocytes were subjected to three different experimental conditions: continuous normoxia (20% O_2) for 12 days; hypoxia (1% O_2) for 4 days followed by normoxia (20% O_2) for 8 days; or continuous hypoxia (1% O_2) for 12 days. Functional assessments were made on day 0; functional, molecular biological and morphological investigations were carried out on day 4 and day 12; functional assessments were made on day 8.

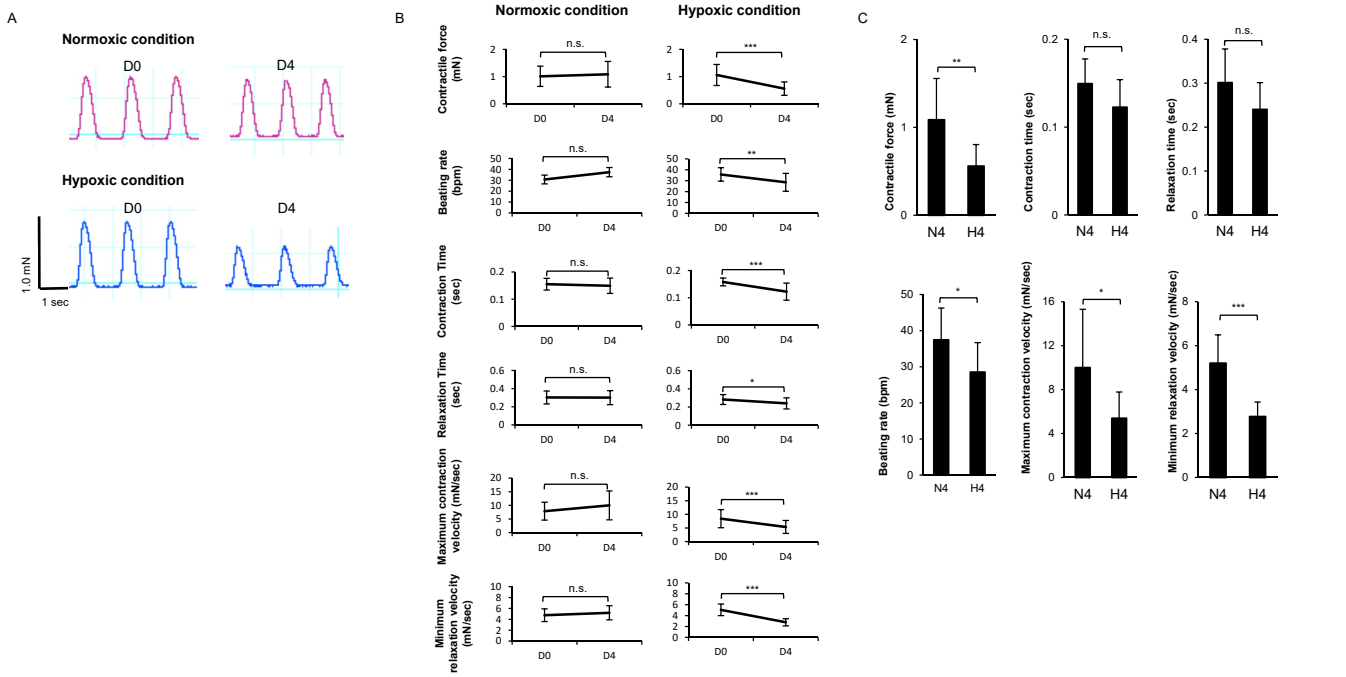

Fig. 2. Effects of hypoxia on the contractile function of iPSC-derived bioengineered cardiac tissue. (A) Representative contractile force traces recorded from a cardiac cell sheet. (B) Cardiac tissues were incubated in normoxic (20% O_2) or hypoxic (1% O_2) conditions for 4 days. Data for contractile force, beating rate, contraction time, relaxation time, maximum contraction velocity and maximum relaxation velocity are shown for day 0 (D0) and day 4 (D4). (C) Comparison of contractile force, beating rate, contraction time, relaxation time, maximum contraction velocity and maximum relaxation velocity on day 4 between the normoxic group (N4) and hypoxic group (H4). Data in (B) and (C) are presented as the mean ± SD of a minimum of 7 preparations. *$P < 0.05$, **$P < 0.01$, ***$P < 0.001$.

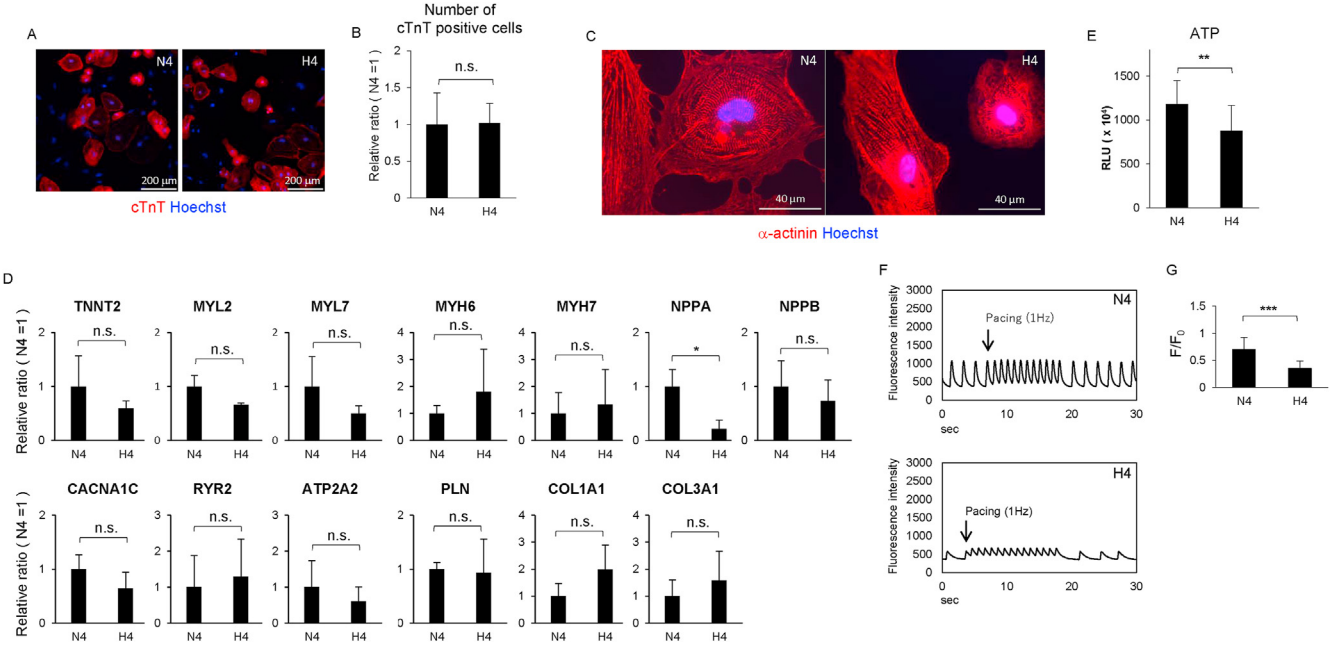

Fig. 3. Morphological and molecular biological changes induced by hypoxia. (A–E) hiPSC-CMs were incubated in normoxic (20% O_2; N4) or hypoxic (1% O_2; H4) conditions for 4 days. (A) Representative images of cTnT-positive cardiomyocytes. Nuclei were labeled with Hoechst. Bars, 200 μm. (B) The number of cTnT-positive cells in 49 fields (7 × 7) was calculated for each time point. The number of cTnT-positive cells in each group was normalized to the mean value of the N4 group (10 biological repeats). (C) Representative images showing sarcomere structure. Cells were stained with α-actinin, and nuclei were labeled with Hoechst. Bars, 40 μm. (D) The mRNA expressions of various genes in cardiomyocytes. Data are shown as the mean ± SD of 3 biological repeats and are normalized to the mean value of the N4 group. (E) Cellular ATP levels in cardiomyocytes. Data are shown as the mean ± SD of 14 biological repeats. RLU: relative light units. (F, G) Cardiac spheroids were cultured for the assigned periods. (F) Representative Ca^{2+} transients recorded from cardiac spheroids. (G) The amplitudes of Ca^{2+} transients measured in cells loaded with fluo-8. Data for F/F_0 (peak fluorescence divided by baseline fluorescence) are presented as the mean ± SD. *$P < 0.05$, **$P < 0.01$, ***$P < 0.001$.

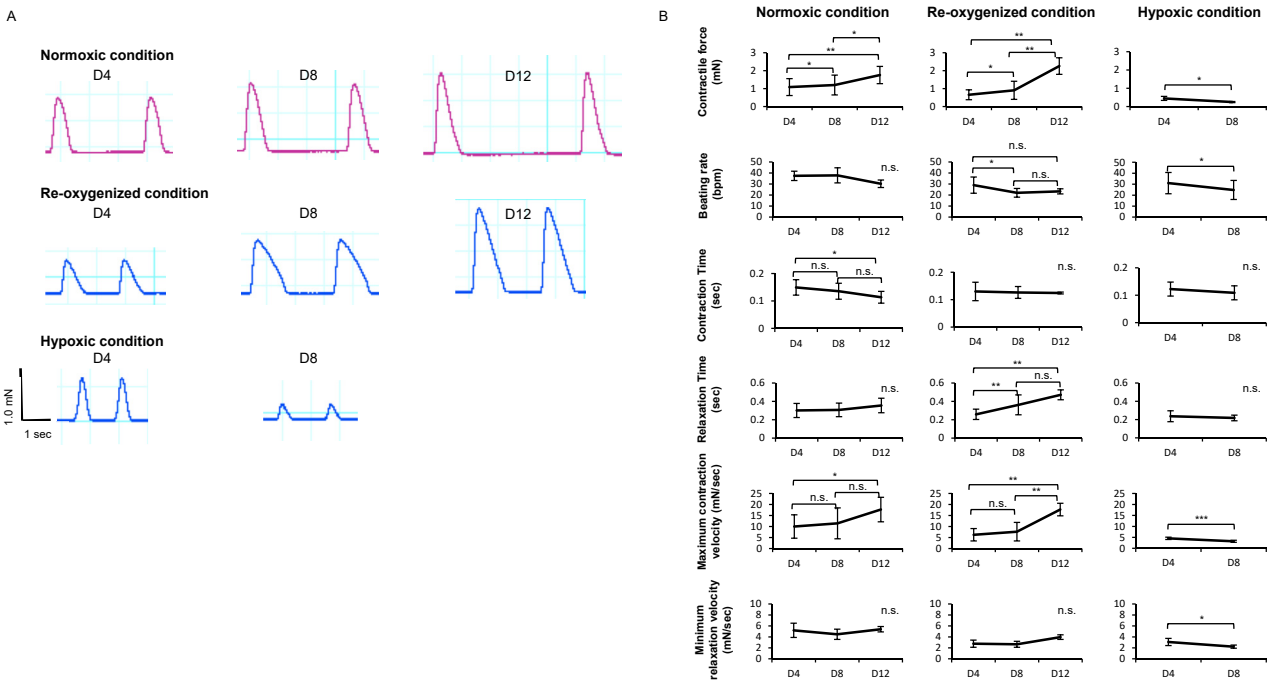

Fig. 4. Effects of continuous normoxia, hypoxia/re-oxygenation and continuous hypoxia on the contractile function of iPSC-derived bioengineered cardiac tissue. Cardiac tissues were maintained under three conditions: continuous normoxia (20% O_2) for 12 days; hypoxia (1% O_2) for 4 days followed by normoxia (20% O_2) for 8 days; or continuous hypoxia (1% O_2) for 12 days. (A) Representative contractile force traces for day 4 (D4), day 8 (D8) and day 12 (D12). (B) Comparison of contraction time, relaxation time, contractile force, beating rate, maximum contraction velocity and maximum relaxation velocity between day 4 (D4), day 8 (D8) and day 12 (D12) for each experimental condition. Data are presented as the mean ± SD of 6 preparations. (C) Comparison of contractile force, beating rate, contraction time, relaxation time, maximum contraction velocity and maximum relaxation velocity on day 12 between the normoxia group (NN12) and hypoxia/normoxia group (HN12). Data are presented as the mean ± SD of 6 preparations. *$P < 0.05$, **$P < 0.01$, ***$P < 0.001$.

maximum relaxation velocity remained significantly suppressed after re-oxygenation compared with the continuous normoxia group (Fig. 4C). These findings imply that hypoxia/re-oxygenation might lead to an impairment of relaxation (i.e. diastolic dysfunction).

Next, we examined the mechanisms of contractile force recovery after re-oxygenation of bioengineered cardiac tissue. The number of cTnT-positive cells did not differ between hiPSC-CMs cultured for 12 days under hypoxic/re-oxygenized conditions and those cultured under continuous normoxia (Fig. 5A and B), indicating little effect of hypoxia/re-oxygenation on cell death. Furthermore, sarcomeric structure was maintained after re-oxygenation (Fig. 5C). Comparisons of the mRNA expressions of 13 genes on day 12 (Fig. 5E) revealed that hypoxia/re-oxygenation induced a significant up-regulation of the gene for phospholamban (*PLN*) as compared with the continuous normoxia group ($P < 0.05$). Thus, hypoxia/re-oxygenation led to an increase in the expression level of a protein that plays an important role in the regulation of cardiomyocyte Ca^{2+} homeostasis, contraction and relaxation. Although there also appeared to be a trend toward increased mRNA expressions of several other genes, including those encoding cTnT (*TNNT2*), myosin light chain-2 (*MYL2*), myosin light chain-7 (*MYL7*), myosin heavy chain-6 (*MYH6*), myosin heavy chain-7 (*MYH7*), natriuretic peptide precursor A (*NPPA*) and subunit α1C of the voltage-gated L-type Ca^{2+} channel (*CACNA1C*), statistical significance was not attained (Fig. 5D). The cellular ATP level on day 8 was not significantly different between the hypoxia/re-oxygenation group and continuous normoxia group (Fig. 5E). Since hypoxia for 4 days induced a fall in ATP level (Fig. 3E), this indicates that restoration of normal oxygen levels after hypoxia resulted in normalization of ATP levels within 4 days. The magnitude of the intracellular Ca^{2+} transient was well maintained in the continuous normoxia group between days 4 and 12 (Fig. 5G). In hiPSC-CMs subjected to hypoxia for 4 days, re-oxygenation resulted in a recovery in the magnitude of the Ca^{2+} transient at days 8 and 12 ($P < 0.01$ vs. day 4; Fig. 5H) such that the magnitude of the Ca^{2+} transient at day 12 did not differ significantly between the hypoxia/re-oxygenation group and continuous normoxia group (Fig. 5I).

4. Discussion

The objective of this research was to develop a model system using bioengineered hiPSC-derived cardiac tissue that could be used to investigate the effects of hypoxia and re-oxygenation on contractile function and explore the underlying mechanisms. The main findings were as follows: 1) hypoxia for 4 days resulted in significant decreases in contractile force, maximum contraction velocity, maximum relaxation velocity and Ca^{2+} transient amplitude; 2) hypoxia had little or no effect on the number of cells; 3) hypoxia was associated with a reduction in cellular ATP level; 4) hypoxia resulted in down-regulated expression of the gene encoding natriuretic peptide precursor A (*NPPA*); 5) hypoxia for 4 days followed by re-oxygenation for 8 days was associated with progressive increases in contractile force, maximum contraction velocity and relaxation time, whereas maximum relaxation velocity did not recover; 6) Ca^{2+} transient magnitude, cell number, sarcomere structure and ATP level after re-oxygenation were similar to those observed in the continuous normoxia group; and 7) hypoxia/re-oxygenation resulted in up-regulated expression of the gene encoding *PLN*. Taken together, these findings indicate that we have successfully generated a model system that may be suitable for the study of hypoxia/re-oxygenation in human cardiac tissue. Notably, hypoxia for 4 days followed by re-oxygenation for 8 days resulted in a recovery of contractile force but not maximum relaxation

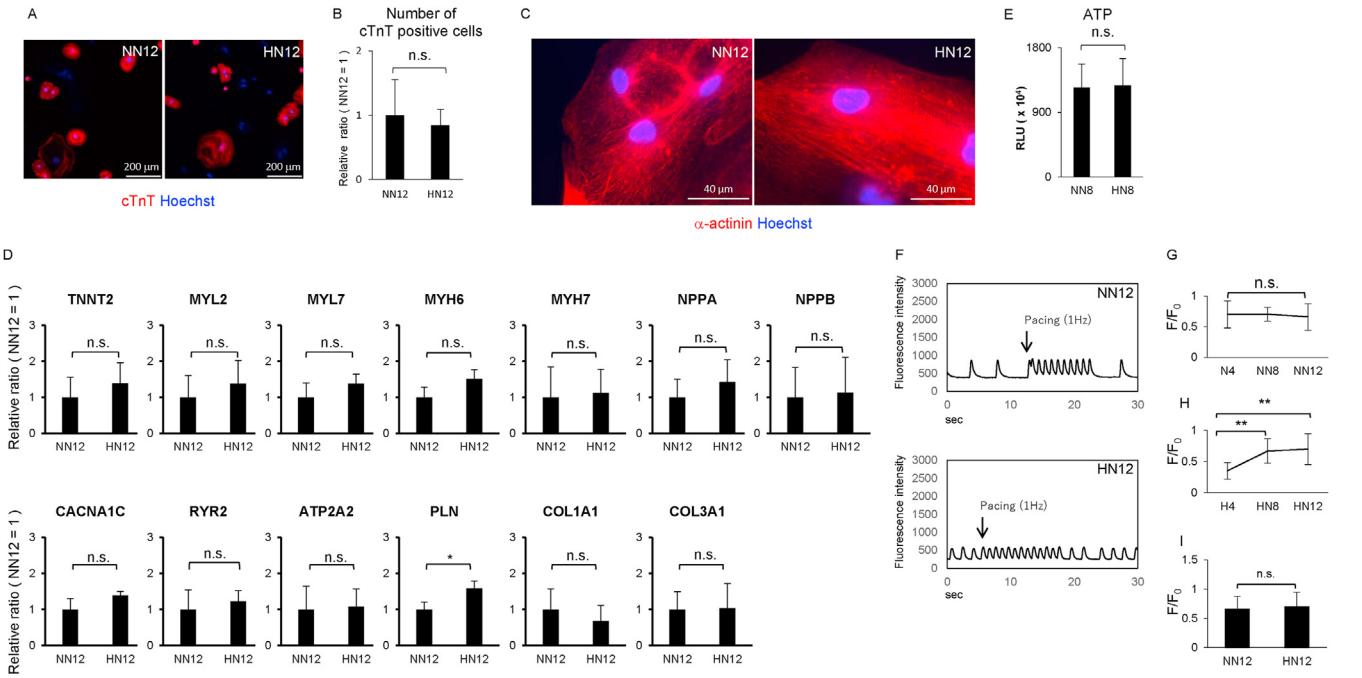

Fig. 5. Morphological and molecular biological changes induced by hypoxia/re-oxygenation. (A–E) hiPSC-CMs were incubated under normoxic conditions (20% O_2) for 12 days (NN12) or hypoxic conditions (1% O_2) for 4 days followed by normoxic conditions (20% O_2) for 8 days (HN12). (A) Representative images of cTnT-positive cardiomyocytes. Nuclei were labeled with Hoechst. Bars, 200 μm. (B) The number of cTnT-positive cells in 49 fields (7 × 7) was calculated for each time point. The number of cardiomyocytes in each group was normalized to the mean value of the NN12 group. (C) Representative images showing sarcomere structure. Cells were stained with α-actinin, and nuclei were labeled with Hoechst. Bars, 40 μm. (D) The mRNA expressions of various genes in cardiomyocytes. Data are shown as the mean ± SD and are normalized to the mean value of the NN12 group. (E) Cellular ATP levels in cardiomyocytes. Data are shown as the mean ± SD. RLU: relative light units. (F–I) Cardiac spheroids were cultured for the assigned periods. (F) Representative Ca^{2+} transients recorded from cardiac spheroids on day 12. (G) The amplitudes of Ca^{2+} transients measured from cells loaded with fluo-8 and exposed to continuous normoxia for 12 days. (H) The amplitudes of Ca^{2+} transients measured from cells loaded with fluo-8 and exposed to hypoxia for 4 days followed by normoxia for 8 days. (I) Comparison of Ca^{2+} transient amplitudes between the NN group and NH group at day 12. Data for F/F_0 (peak fluorescence divided by baseline fluorescence) are presented as the mean ± SD ($n = 16$ for NN and $n = 26$ for NH). $^*P < 0.05$, $^{**}P < 0.01$, $^{***}P < 0.001$.

velocity, suggesting that this protocol may be suitable for use as a preclinical model of heart failure with recovered EF and diastolic dysfunction.

Studying the responses of iPSC-derived cardiac tissue to hypoxia and re-oxygenation may give crucial insights into the mechanisms underlying cardiac damage and heart failure induced by hypoxia and allow research into novel treatment strategies to minimize or even reverse this damage. We found that continuous hypoxia (i.e. a decrease from 20% O_2 to 1% O_2) resulted in progressive reductions in contractile force, maximum contraction velocity, maximum relaxation velocity, relaxation time and beating rate, and no contractions were evident after 12 days. This is consistent with published studies in animal models reporting decreases in the rate and force of contraction in heart tissue exposed to hypoxia [26–28]. Hypoxia for 4 days also caused a suppression in the magnitude of the Ca^{2+} transient, implying dysfunction of intracellular Ca^{2+} homeostasis; this is also in agreement with previous research [29]. Chronic hypoxia for 4 days did not lead to a change in the number of cells (i.e. cell death). However, chronic hypoxia was associated with a fall in ATP levels, suggesting that the iPSC-CMs were not able to fully adapt to the hypoxic challenge and maintain their ATP levels through decreases in contractile force and oxygen consumption. A previous study of spontaneously contracting embryonic cardiomyocytes reported a significant reduction in contractile activity and a slowing of relaxation (in agreement with our findings) that was not associated with a depletion of ATP or phosphocreatine stores [30]. Hypoxia in chick embryonic cardiomyocytes and rat adult cardiomyocytes results in enhanced glucose utilization and increased lactate production [27,30], implying a switch to an anaerobic pattern of metabolism that would help to maintain cellular levels of ATP during hypoxia. It is possible that iPSC-CMs are less able to compensate for hypoxia by switching to anaerobic metabolism, which may contribute to their sensitivity to hypoxia and nutrient deprivation [31]. It has been reported that extracellular ATP enhances the intracellular Ca^{2+} transient and increase the amplitude of contraction in single rat cardiomyocytes [32]. Conversely, the increase of cytoplasmic Ca^{2+} has also been reported to induce ATP production through the increase of mitochondrial Ca^{2+} concentration and FAD-glycerol phosphate dehydrogenase [33]. Therefore, impaired ATP production and decreased intracellular Ca^{2+} transient might synergistically affect the systolic and relaxation function in the hypoxic condition. On the other hand, when systolic function is recovered after re-oxygenation, ATP production levels and Ca^{2+} transient were recovered to those in the continuous normoxic condition, which are consistent with the evidences that ATP production and Ca^{2+} transient influence each other [32,33].

It is well established that myocardial reperfusion after hypoxia can itself cause cardiomyocyte death [34]. For example, 48 h of hypoxia was found not to cause apoptosis of rat cardiomyocytes, whereas 24 h of hypoxia followed by 24 h of re-oxygenation induced substantial apoptosis of cells [35]. In the present study, re-oxygenation after 4 days of hypoxia was not associated with cell death but instead led to a progressive recovery in contractile function, Ca^{2+} transient amplitude and ATP level. This suggests that the iPSC-CMs utilized in this research were able to tolerate the hypoxic challenge and recover much of their function after re-oxygenation. The present findings contrast with those of other investigations demonstrating substantial cardiomyocyte apoptosis during prolonged hypoxia [36] or after hypoxia/re-oxygenation

[35]. One possible explanation for this apparent discrepancy is that the iPSC-CMs in this study were exposed only to hypoxia and not to acidosis or a build-up of other metabolites, which would occur during ischemia-reperfusion injury *in vivo*. For example, it has been shown that apoptosis of rat neonatal cardiomyocytes only occurred when chronic hypoxia was accompanied by acidosis [35]. Furthermore, a previous investigation reported that iPSC-CMs were resistant to hypoxia alone (apoptosis occurred in ~5% of cells) but sensitive to hypoxia in combination with acidosis (apoptosis occurred in ~60% of cells) [37]. A second possible explanation is that cell maturity may affect the sensitivity to hypoxia/re-oxygenation. Indeed, it has been demonstrated that maturation of iPSC-CMs increases their susceptibility to hypoxia/re-oxygenation [37]. These possibilities have important implications with regard to the use of iPSC-derived cardiac cell sheets as a model of chronic cardiac hypoxia/ischemia. Thus, the present series of experiments will need to be extended to examine the sensitivity of iPSC-derived cardiac cell sheets to hypoxia in the presence of acidosis and other metabolites known to accumulate during myocardial ischemia and to explore the effects of cell maturation on the response to hypoxia/re-oxygenation.

Although further refinement of our model of hypoxia/re-oxygenation may improve its validity, certain observations made in the present study indicate that iPSC-derived cardiac cell sheets may have potential as a preclinical model of human heart failure with recovered EF and diastolic dysfunction. As shown in Fig. 4C, cardiac tissue contractile force recovered after re-oxygenation to reach a level comparable to that observed under continuous normoxic conditions, whereas maximum relaxation velocity remained suppressed following hypoxia/re-oxygenation when compared with the continuous normoxia group. EF is a powerful predictor of clinical outcome in patients with heart failure [38,39], but a recent study indicated that the response of the EF to treatment further predicts outcomes in patients [40]. However, since it has been reported that left ventricular volume is larger in patients with heart failure and recovered EF than in patients with HFpEF [41] and that withdrawal of pharmacotherapy leads to relapse in patients with heart failure and dilated cardiomyopathy [8], some maladaptive changes may persist even after functional recovery. In this study, we observed that maximum relaxation velocity was decreased after 4 days of hypoxia and did not improve after 8 days of re-oxygenation, suggesting that contractile function recovers promptly after re-oxygenation but that recovery of relaxation function might be delayed. Human cardiac tissue model might be possible to distinguish between HFrEF and HFpEF. Cell death due to several conditions including ischemia, inflammation and prolong period overload, and subsequent fibrosis are main causes of HFrEF, while cardiomyocyte is survived, in principle, but relaxation dysfunction of cardiomyocyte and fibrosis-mediated diastolic dysfunction are main causes of HFpEF. In the present study, we did not observe cardiomyocyte loss at 4 days in hypoxia and at 8 days after re-oxygenation, while relaxation dysfunction, but not systolic dysfunction, was observed at 8 days after re-oxygenation. Therefore, the cardiac tissue model shown in the present study might be compatible for HFpEF rather than HFrEF. It has been reported that diastolic dysfunction remains impaired even after the ischemia is released in patients with acute myocardial infarction [42] and diastolic dysfunction is prolonged in patients with heart failure with improved ejection fraction [43], suggesting that diastolic functional recovery might be delayed in the pathological conditions. Although the prolong period pressure overload is well known to induce systolic dysfunction through cardiomyocyte apoptosis and fibrosis in accompanied with the insufficient angiogenesis [44], intermittent pressure overload has been reported to induce diastolic dysfunction in accompanied with the insufficient angiogenesis (vascular rarefaction) without fibrosis [45], suggesting that intermittent insufficient blood flow might be one of causes of diastolic dysfunction. Since daily variation of blood pressure is well known phenomena, intermittent pressure overload might be more compatible to account for the pathological conditions in the early phase of hypertensive heart disease. Furthermore, left ventricular diastolic dysfunction without left ventricular hypertrophy has been advocated as an initial phase in the transition from hypertension to heart failure [46]. Herein, human iPSC-derived cardiac tissue after hypoxia/re-oxygenation might recapitulate some pathological conditions of HFpEF.

Previous investigations have described alterations in cardiac gene expression patterns in response to hypoxia and re-oxygenation [47–49]. Data are very limited regarding hypoxia-induced gene expression changes in hiPSC-CMs. However, it was recently reported that 937 proteins were up-regulated or down-regulated in iPSC-CMs exposed to hypoxia or hypoxia/re-oxygenation, including proteins associated with the mitochondrial proton-transporting ATP synthase complex and cardiac muscle contraction [50]. In the present study, hypoxia resulted in a significant down-regulation in the expression of the *NPPA* gene. Atrial natriuretic peptide (ANP), the active product of the *NPPA* gene, plays an important physiological role in the regulation of blood volume and pressure [51]. ANP is upregulated in ischemic and dilated cardiomyopathy [52], and it is thought that ANP plays a role in countering the development of heart failure [53]. Contrary to the present findings, previous investigations have reported that ANP levels are increased in response to ischemia [54,55]. The discrepancy may in part be due to the fact that the elevation in ANP in response to cardiac hypoxia *in vivo* is mediated by endothelin [56], which would not be produced in iPSC-derived cardiac cell sheets due to a lack of vascular endothelial cells. Since ANP is widely considered to be cardioprotective in the setting of cardiac hypertrophy and heart failure, the reduced mRNA expression of the *NPPA* gene in this study would likely have detrimental effects in bioengineered cardiac cell sheets during prolonged hypoxia.

In this study, hypoxia/re-oxygenation resulted in up-regulation of the gene encoding PLN, which influences the force of contraction and rate of relaxation by regulating Ca^{2+} uptake into the sarcoplasmic reticulum by sarco/endoplasmic reticulum Ca^{2+} ATPase (SERCA)-2 [57,58]. Interestingly, this contrasts with animal studies reported in the literature, which have described a decrease in the expression of PLN in response to ischemia-reperfusion [59–61]. Since ablation of PLN has been shown to exacerbate ischemia-reperfusion injury [62,63], it may be that the enhanced expression of PLN in hiPSC-CMs has a beneficial effect. Increased expression of PLN would be expected to inhibit Ca^{2+} uptake into the sarcoplasmic reticulum and thereby slow the rate of relaxation, and this may underlie the prolongation of relaxation observed following hypoxia/re-oxygenation. Nonetheless, the function of PLN is regulated by phosphorylation: dephosphorylated PLN inhibits Ca^{2+} uptake into the sarcoplasmic reticulum by SERCA, but phosphorylation of PLN removes its inhibitory effect on SERCA and thereby enhances Ca^{2+} uptake. Thus, changes in PLN phosphorylation during hypoxia also need to be taken into account. At present, data regarding the phosphorylation status of PLN after ischemia-reperfusion are equivocal [64–66], so this will need to be further examined in future studies. Interestingly, reduced levels of PLN have been measured in animal models of heart failure and dilated cardiomyopathy [67,68], potentially implicating PLN down-regulation in the pathogenesis of these conditions.

One of the merit of the usage of cardiac tissue model and the contractile force measurement is the functional evaluation of whole tissue. The contractile function of cardiac tissue is mediated

by several factors including each cardiomyocyte contraction, action potential propagation velocity and tissue stiffness. And the electrophysiological function affects cardiomyocyte contraction and action potential propagation velocity. In that respect, the contractile phenotypes in hypoxia/re-oxygenation are the additive results of each factor influenced by hypoxia/re-oxygenation and it might be the sensitive assessment indicator to examine the effect of the hypoxia/re-oxygenation. Currently there are few reports on the electrophysiological effects of hypoxia and re-oxygenation in human pluripotent stem cell-derived cardiomyocyte/cardiac tissue, but it has been reported that hypoxia decreases the spontaneous beating rate and delays conduction velocity in mouse embryonic stem cell-derived cardiomyocyte embryoid body [69]. As human iPSC-derived cardiomyocytes have also been widely applied for drug proarrhythmic potential assessment [70], the contribution of each factor including electrophysiological aspect to the contractile phenotype in the hypoxia and re-oxygenation will be clear.

An important aim of future experiments will be to further characterize the hypoxia/re-oxygenation model described in this study and establish the molecular mechanisms that underlie the functional changes that develop during hypoxia and the recovery that occurs during re-oxygenation. In particular, it will be necessary to validate the system as a potential model of heart failure with recovered EF and diastolic dysfunction. Possible approaches to refining and improving the model will also be explored, such as enhancing the maturation of iPSC-CMs, improving their alignment and undertaking co-culture with other supporting cells. Another future objective will be to utilize this methodology to create preclinical models of inherited cardiomyopathy and drug-induced cardiomyopathy. This can be achieved by harvesting iPSCs from patients with inherited diseases such as hypertrophic cardiomyopathy and dilated cardiomyopathy, and also cultivating iPSCs-derived cardiac tissues with anti-cancer drugs such as doxorubicin and trastuzumab.

5. Conclusions

The findings of this study indicate that we have successfully generated a model system that may be suitable for the study of hypoxia/re-oxygenation. Further understanding of the molecular mechanisms underlying the functional recovery of cardiac tissue after re-oxygenation might provide us with new insights into heart failure with recovered EF and preserved EF.

Declaration of competing interest

There are potential competing interests. Tatsuya Shimizu was a member of the scientific advisory board of CellSeed Inc. and is a shareholder of CellSeed Inc. Tokyo Women's Medical University receives a research fund from CellSeed Inc. for the practical application of cell sheet engineering. Katsuhisa Matsuura and Tatsuya Shimizu are inventors of bioreactor systems. The other authors declare no conflicts of interest.

Acknowledgments

We thank K. Sugiyama, H. Miyatake and M. Tejima for their excellent technical assistance. This research was supported by AMED (grant number 18bm0804010h0102) and Mitsukoshi Health and Welfare Foundation. We thank OXMEDCOMMS (www.oxmedcomms.com) assistance in the preparation of this article.

References

[1] Muiesan ML, Paini A, Agabiti Rosei C, Bertacchini F, Stassaldi D, Salvetti M. Current pharmacological therapies in heart failure patients. High Blood Press Cardiovasc Prev 2017;24:107–14.
[2] Gordin JS, Fonarow GC. New medications for heart failure. Trends Cardiovasc Med 2016;26:485–92.
[3] Metra M, Teerlink JR. Heart failure. Lancet 2017;390:1981–95.
[4] Ponikowski P, Voors AA, Anker SD, Bueno H, Cleland JGF, Coats AJS, et al. 2016 ESC Guidelines for the diagnosis and treatment of acute and chronic heart failure: the Task Force for the diagnosis and treatment of acute and chronic heart failure of the European Society of Cardiology (ESC) Developed with the special contribution of the Heart Failure Association (HFA) of the ESC. Eur Heart J 2016;37:2129–200.
[5] Shah KS, Xu H, Matsouaka RA, Bhatt DL, Heidenreich PA, Hernandez AF, et al. Heart failure with preserved, borderline, and reduced ejection fraction: 5-year outcomes. J Am Coll Cardiol 2017;70:2476–86.
[6] Lupon J, Diez-Lopez C, de Antonio M, Domingo M, Zamora E, Moliner P, et al. Recovered heart failure with reduced ejection fraction and outcomes: a prospective study. Eur J Heart Fail 2017;19:1615–23.
[7] Rastogi A, Novak E, Platts AE, Mann DL. Epidemiology, pathophysiology and clinical outcomes for heart failure patients with a mid-range ejection fraction. Eur J Heart Fail 2017;19:1597–605.
[8] Halliday BP, Wassall R, Lota AS, Khalique Z, Gregson J, Newsome S, et al. Withdrawal of pharmacological treatment for heart failure in patients with recovered dilated cardiomyopathy (TRED-HF): an open-label, pilot, randomised trial. Lancet 2019;393:61–73.
[9] Yamamoto W, Asakura K, Ando H, Taniguchi T, Ojima A, Uda T, et al. Electrophysiological characteristics of human iPSC-derived cardiomyocytes for the assessment of drug-induced proarrhythmic potential. PLoS One 2016;11:e0167348.
[10] Wen JY, Wei CY, Shah K, Wong J, Wang C, Chen HS. Maturation-based model of arrhythmogenic right ventricular dysplasia using patient-specific induced pluripotent stem cells. Circ J 2015;79:1402–8.
[11] Sun N, Yazawa M, Liu J, Han L, Sanchez-Freire V, Abilez OJ, et al. Patient-specific induced pluripotent stem cells as a model for familial dilated cardiomyopathy. Sci Transl Med 2012;4:130ra47.
[12] Sharma A, Marceau C, Hamaguchi R, Burridge PW, Rajarajan K, Churko JM, et al. Human induced pluripotent stem cell-derived cardiomyocytes as an in vitro model for coxsackievirus B3-induced myocarditis and antiviral drug screening platform. Circ Res 2014;115:556–66.
[13] Smith AS, Macadangdang J, Leung W, Laflamme MA, Kim DH. Human iPSC-derived cardiomyocytes and tissue engineering strategies for disease modeling and drug screening. Biotechnol Adv 2017;35:77–94.
[14] Parsa H, Ronaldson K, Vunjak-Novakovic G. Bioengineering methods for myocardial regeneration. Adv Drug Deliv Rev 2016;96:195–202.
[15] Yang J, Yamato M, Shimizu T, Sekine H, Ohashi K, Kanzaki M, et al. Reconstruction of functional tissues with cell sheet engineering. Biomaterials 2007;28:5033–43.
[16] Owaki T, Shimizu T, Yamato M, Okano T. Cell sheet engineering for regenerative medicine: current challenges and strategies. Biotechnol J 2014;9:904–14.
[17] Egami M, Haraguchi Y, Shimizu T, Yamato M, Okano T. Latest status of the clinical and industrial applications of cell sheet engineering and regenerative medicine. Arch Pharm Res (Seoul) 2014;37:96–106.
[18] Matsuura K, Wada M, Shimizu T, Haraguchi Y, Sato F, Sugiyama K, et al. Creation of human cardiac cell sheets using pluripotent stem cells. Biochem Biophys Res Commun 2012;425:321–7.
[19] Seta H, Matsuura K, Sekine H, Yamazaki K, Shimizu T. Tubular cardiac tissues derived from human induced pluripotent stem cells generate pulse pressure in vivo. Sci Rep 2017;7:45499.
[20] Sasaki D, Matsuura K, Seta H, Haraguchi Y, Okano T, Shimizu T. Contractile force measurement of human induced pluripotent stem cell-derived cardiac cell sheet-tissue. PLoS One 2018;13:e0198026.
[21] Lee S, Sasaki D, Kim D, Mori M, Yokota T, Lee H, et al. Ultrasoft electronics to monitor dynamically pulsing cardiomyocytes. Nat Nanotechnol 2019;14:156–60.
[22] Chen T, Vunjak-Novakovic G. Human tissue-engineered model of myocardial ischemia-reperfusion injury. Tissue Eng Part A 2019;25:711–24.
[23] Takahashi K, Tanabe K, Ohnuki M, Narita M, Ichisaka T, Tomoda K, et al. Induction of pluripotent stem cells from adult human fibroblasts by defined factors. Cell 2007;131:861–72.
[24] Matsuura K, Seta H, Haraguchi Y, Alsayegh K, Sekine H, Shimizu T, et al. TRPV-1-mediated elimination of residual iPS cells in bioengineered cardiac cell sheet tissues. Sci Rep 2016;6:21747.
[25] Clements M, Thomas N. High-throughput multi-parameter profiling of electrophysiological drug effects in human embryonic stem cell derived cardiomyocytes using multi-electrode arrays. Toxicol Sci 2014;140:445–61.
[26] Anttila K, Streng T, Pispa J, Vainio M, Nikinmaa M. Hypoxia exposure and B-type natriuretic peptide release from Langendorff heart of rats. Acta Physiol (Oxf) 2017;220:28–35.
[27] Silverman HS, Wei S, Haigney MC, Ocampo CJ, Stern MD. Myocyte adaptation to chronic hypoxia and development of tolerance to subsequent acute severe hypoxia. Circ Res 1997;80:699–707.

[28] Duranteau J, Chandel NS, Kulisz A, Shao Z, Schumacker PT. Intracellular signaling by reactive oxygen species during hypoxia in cardiomyocytes. J Biol Chem 1998;273:11619–24.
[29] Martewicz S, Michielin F, Serena E, Zambon A, Mongillo M, Elvassore N. Reversible alteration of calcium dynamics in cardiomyocytes during acute hypoxia transient in a microfluidic platform. Integr Biol (Camb) 2012;4:153–64.
[30] Budinger GR, Chandel N, Shao ZH, Li CQ, Melmed A, Becker LB, et al. Cellular energy utilization and supply during hypoxia in embryonic cardiac myocytes. Am J Physiol 1996;270:L44–53.
[31] Brodarac A, Saric T, Oberwallner B, Mahmoodzadeh S, Neef K, Albrecht J, et al. Susceptibility of murine induced pluripotent stem cell-derived cardiomyocytes to hypoxia and nutrient deprivation. Stem Cell Res Ther 2015;6:83.
[32] Danziger RS, Raffaeli S, Moreno-Sanchez R, Sakai M, Capogrossi MC, Spurgeon HA, et al. Extracellular ATP has a potent effect to enhance cytosolic calcium and contractility in single ventricular myocytes. Cell Calcium 1988;9:193–9.
[33] Denton RM. Regulation of mitochondrial dehydrogenases by calcium ions. Biochim Biophys Acta 2009;1787:1309–16.
[34] Hausenloy DJ, Yellon DM. Myocardial ischemia-reperfusion injury: a neglected therapeutic target. J Clin Invest 2013;123:92–100.
[35] Webster KA, Discher DJ, Kaiser S, Hernandez O, Sato B, Bishopric NH. Hypoxia-activated apoptosis of cardiac myocytes requires reoxygenation or a pH shift and is independent of p53. J Clin Invest 1999;104:239–52.
[36] Kang PM, Haunstetter A, Aoki H, Usheva A, Izumo S. Morphological and molecular characterization of adult cardiomyocyte apoptosis during hypoxia and reoxygenation. Circ Res 2000;87:118–25.
[37] Hidalgo A, Glass N, Ovchinnikov D, Yang SK, Zhang XL, Mazzone S, et al. Modelling ischemia-reperfusion injury (IRI) in vitro using metabolically matured induced pluripotent stem cell-derived cardiomyocytes. APL Bioeng 2018;2.
[38] Solomon SD, Anavekar N, Skali H, McMurray JJ, Swedberg K, Yusuf S, et al. Influence of ejection fraction on cardiovascular outcomes in a broad spectrum of heart failure patients. Circulation 2005;112:3738–44.
[39] Smith DH, Johnson ES, Thorp ML, Yang X, Petrik A, Platt RW, et al. Predicting poor outcomes in heart failure. Perm J 2011;15:4–11.
[40] Gulati G, Udelson JE. Heart failure with improved ejection fraction: is it possible to escape one's past? JACC Heart Fail 2018;6:725–33.
[41] Punnoose LR, Givertz MM, Lewis EF, Pratibhu P, Stevenson LW, Desai AS. Heart failure with recovered ejection fraction: a distinct clinical entity. J Card Fail 2011;17:527–32.
[42] Cerisano G, Bolognese L, Buonamici P, Valenti R, Carrabba N, Dovellini EV, et al. Prognostic implications of restrictive left ventricular filling in reperfused anterior acute myocardial infarction. J Am Coll Cardiol 2001;37:793–9.
[43] Park CS, Park JJ, Mebazaa A, Oh IY, Park HA, Cho HJ, et al. Characteristics, outcomes, and treatment of heart failure with improved ejection fraction. J Am Heart Assoc 2019;8:e011077.
[44] Sano M, Minamino T, Toko H, Miyauchi H, Orimo M, Qin Y, et al. p53-induced inhibition of Hif-1 causes cardiac dysfunction during pressure overload. Nature 2007;446:444–8.
[45] Perrino C, Naga Prasad SV, Mao L, Noma T, Yan Z, Kim HS, et al. Intermittent pressure overload triggers hypertrophy-independent cardiac dysfunction and vascular rarefaction. J Clin Invest 2006;116:1547–60.
[46] Messerli FH, Rimoldi SF, Bangalore S. The transition from hypertension to heart failure: contemporary update. JACC Heart Fail 2017;5:543–51.
[47] Pavo N, Lukovic D, Zlabinger K, Zimba A, Lorant D, Goliasch G, et al. Sequential activation of different pathway networks in ischemia-affected and non-affected myocardium, inducing intrinsic remote conditioning to prevent left ventricular remodeling. Sci Rep 2017;7:43958.
[48] Kim HK, Kang SW, Jeong SH, Kim N, Ko JH, Bang H, et al. Identification of potential target genes of cardioprotection against ischemia-reperfusion injury by express sequence tags analysis in rat hearts. J Cardiol 2012;60:98–110.
[49] Muehlschlegel JD, Christodoulou DC, McKean D, Gorham J, Mazaika E, Heydarpour M, et al. Using next-generation RNA sequencing to examine ischemic changes induced by cold blood cardioplegia on the human left ventricular myocardium transcriptome. Anesthesiology 2015;122:537–50.
[50] Pinho J, Scrimgeour NR, Stolen T, Solvang-Garten K, Sharma A, Fonseca DM, et al. Modeling of cardiac ischaemia and reperfusion injury: a human-based in vitro model using iPS-derived cardiomyocytes. Eur Heart J 2017;38:229–30.
[51] Potter LR, Yoder AR, Flora DR, Antos LK, Dickey DM. Natriuretic peptides: their structures, receptors, physiologic functions and therapeutic applications. Handb Exp Pharmacol 2009;191:341–66.
[52] Tarazon E, Rosello-Lleti E, Rivera M, Ortega A, Molina-Navarro MM, Trivino JC, et al. RNA sequencing analysis and atrial natriuretic peptide production in patients with dilated and ischemic cardiomyopathy. PLoS One 2014;9:e90157.
[53] Maisel AS, Duran JM, Wettersten N. Natriuretic peptides in heart failure: atrial and B-type natriuretic peptides. Heart Fail Clin 2018;14:13–25.
[54] Yamada J, Fujimori K, Ishida T, Sanpei M, Honda S, Sato A. Plasma endothelin-1 and atrial natriuretic peptide levels during prolonged (24-h) non-acidemic hypoxemia in fetal goats. J Matern Fetal Med 2001;10:409–13.
[55] Zhou C, Zhuang J, Zhang X, Zhang J. Changes in atrial natriuretic peptide levels during cardiac bypass in the fetal goat. Artif Organs 2008;32:956–61.
[56] Dietz JR. Mechanisms of atrial natriuretic peptide secretion from the atrium. Cardiovasc Res 2005;68:8–17.
[57] Shaikh SA, Sahoo SK, Periasamy M. Phospholamban and sarcolipin: are they functionally redundant or distinct regulators of the Sarco(Endo)Plasmic Reticulum Calcium ATPase? J Mol Cell Cardiol 2016;91:81–91.
[58] Haghighi K, Bidwell P, Kranias EG. Phospholamban interactome in cardiac contractility and survival: a new vision of an old friend. J Mol Cell Cardiol 2014;77:160–7.
[59] Takeo S, Nasa Y, Tanonaka K, Yamaguchi F, Yabe K, Hayashi H, et al. Role of cardiac renin-angiotensin system in sarcoplasmic reticulum function and gene expression in the ischemic-reperfused heart. Mol Cell Biochem 2000;212:227–35.
[60] Temsah RM, Kawabata K, Chapman D, Dhalla NS. Preconditioning prevents alterations in cardiac SR gene expression due to ischemia-reperfusion. Am J Physiol Heart Circ Physiol 2002;282:H1461–6.
[61] Temsah RM, Kawabata K, Chapman D, Dhalla NS. Modulation of cardiac sarcoplasmic reticulum gene expression by lack of oxygen and glucose. FASEB J 2001;15:2515–7.
[62] Wolska BM, Stojanovic MO, Luo W, Kranias EG, Solaro RJ. Effect of ablation of phospholamban on dynamics of cardiac myocyte contraction and intracellular Ca^{2+}. Am J Physiol 1996;271:C391–7.
[63] Cross HR, Kranias EG, Murphy E, Steenbergen C. Ablation of PLB exacerbates ischemic injury to a lesser extent in female than male mice: protective role of NO. Am J Physiol Heart Circ Physiol 2003;284:H683–90.
[64] Inserte J, Hernando V, Ruiz-Meana M, Poncelas-Nozal M, Fernandez C, Agullo L, et al. Delayed phospholamban phosphorylation in post-conditioned heart favours Ca^{2+} normalization and contributes to protection. Cardiovasc Res 2014;103:542–53.
[65] Shintani-Ishida K, Yoshida K. Ischemia induces phospholamban dephosphorylation via activation of calcineurin, PKC-alpha, and protein phosphatase 1, thereby inducing calcium overload in reperfusion. Biochim Biophys Acta 2011;1812:743–51.
[66] Vittone L, Mundina-Weilenmann C, Said M, Ferrero P, Mattiazzi A. Time course and mechanisms of phosphorylation of phospholamban residues in ischemia-reperfused rat hearts. Dissociation of phospholamban phosphorylation pathways. J Mol Cell Cardiol 2002;34:39–50.
[67] Wang L, Zhang SJ, Li L, Lan C, Zhang R, Liu ZH. [Abnormal calcium re-uptake in myocardium sarcoplasmic reticulum in rabbits with heart failure and the influencing factors]. Sheng Li Xue Bao 2014;66:483–8.
[68] Yokoe S, Asahi M. Phospholamban is downregulated by pVHL-mediated degradation through oxidative stress in failing heart. Int J Mol Sci 2017;18.
[69] Wenzel F, Dittrich M, Hescheler J, Grote J. Hypoxia influences generation and propagation of electrical activity in embryonic cardiomyocyte clusters. Comp Biochem Physiol A Mol Integr Physiol 2002;132:111–5.
[70] Blinova K, Dang Q, Millard D, Smith G, Pierson J, Guo L, et al. International multisite study of human-induced pluripotent stem cell-derived cardiomyocytes for drug proarrhythmic potential assessment. Cell Rep 2018;24:3582–92.